NREL
NATIONAL RENEWABLE ENERGY LABORATORY

Wind Turbine Wake-Redirection Control at the Fishermen's Atlantic City Windfarm

Preprint

M. Churchfield and P. Fleming
National Renewable Energy Laboratory

B. Bulder
Energy Centre of the Netherlands

S. White
Fishermen's Atlantic City Windfarm, LLC

To be presented at the Offshore Technology Conference
Houston, Texas
May 4–7, 2015

NREL is a national laboratory of the U.S. Department of Energy
Office of Energy Efficiency & Renewable Energy
Operated by the Alliance for Sustainable Energy, LLC

This report is available at no cost from the National Renewable Energy Laboratory (NREL) at www.nrel.gov/publications.

Conference Paper
NREL/CP-5000-63575
May 2015

Contract No. DE-AC36-08GO28308

This report is available at no cost from the National Renewable Energy Laboratory (NREL) at www.nrel.gov/publications.

Available electronically at http://www.osti.gov/scitech

Available for a processing fee to U.S. Department of Energy and its contractors, in paper, from:

U.S. Department of Energy
Office of Scientific and Technical Information
P.O. Box 62
Oak Ridge, TN 37831-0062
phone: 865.576.8401
fax: 865.576.5728
email: mailto:reports@adonis.osti.gov

Available for sale to the public, in paper, from:

U.S. Department of Commerce
National Technical Information Service
5285 Port Royal Road
Springfield, VA 22161
phone: 800.553.6847
fax: 703.605.6900
email: orders@ntis.fedworld.gov
online ordering: http://www.ntis.gov/help/ordermethods.aspx

Cover Photos: (left to right) photo by Pat Corkery, NREL 16416, photo from SunEdison, NREL 17423, photo by Pat Corkery, NREL 16560, photo by Dennis Schroeder, NREL 17613, photo by Dean Armstrong, NREL 17436, photo by Pat Corkery, NREL 17721.

NREL prints on paper that contains recycled content.

Wind Turbine Wake-Redirection Control at the Fishermen's Atlantic City Windfarm

Matthew J. Churchfield and Paul Fleming, National Renewable Energy Laboratory
Bernard Bulder, Energy Centre of the Netherlands
Stanley M. White, Fishermen's Atlantic City Windfarm, LLC

Abstract

In this paper, we will present our work towards designing a control strategy to mitigate wind turbine wake effects by redirecting the wakes, specifically applied to the Fishermen's Atlantic City Windfarm, proposed for deployment within the next few years off the shore of Atlantic City, New Jersey. As wind turbines extract energy from the air, they create low-speed wakes that extend behind them. Full wake recovery to the undisturbed wind speed takes a significant distance. In a wind energy plant the wakes of upstream turbines may travel downstream to the next row of turbines, effectively subjecting them to lower wind speeds, meaning these waked turbines will produce less power.

Wakes can be redirected laterally to some degree, though, by applying yaw misalignment to the wake-generating turbine (i.e., not pointing the turbine directly into the wind). Yaw misalignment causes part of the rotor thrust vector to be pointed in the cross-stream direction, deflecting the flow and the wake in that direction. Yaw misalignment reduces power production, but the global increase in wind plant power caused by decreased wake effects creates a net increase in power production. With the increase in power can come an increase in fatigue loads, though, caused by yaw misalignment. However, if misalignment is applied properly, and it is layered with individual blade pitch control, the load increase can be mitigated. To explore the idea of wake redirection, we used high-fidelity computational fluid dynamics.

Our computational fluid dynamics simulations predict that when winds are aligned with the row, which is one of two predominant wind directions, wake-redirection control can create a 10% increase in energy capture efficiency. This means that, for a given wind energy plant's electrical generating capacity, if wake-redirection control were employed, turbines could be more closely spaced, thereby reducing the watersheet area of the wind plant. Likewise, for a given watersheet area, the total electrical generating capacity can be increased.

In this paper, we discuss the concept of wake redirection through wind turbine yaw misalignment and present our computational fluid dynamics results of the Fishermen's Atlantic City Windfarm project. We also discuss the implications of wake-redirection control on annual energy production and fatigue loads, as well as plans to implement wake-redirection control at Fishermen's Atlantic City Windfarm when it is operational—something not done before at a commercial wind plant.

Introduction

When offshore turbines are placed in large arrays they generally experience an overall loss in energy production and an increase in their structural loading compared to isolated installations where turbines are undisturbed by adjacent turbines. These array effects increase the total cost of energy because less energy is produced and the maintenance costs are greater. The understanding of turbine wakes and the complex interaction of turbines with the atmosphere is a relatively new area of science within the wind industry. Current industry tools to model these interactions are often inaccurate under certain atmospheric conditions. New higher fidelity models are being developed but they have not yet been fully validated with robust field measurements.

This paper is summarizes our latest efforts to simulate the wake effects in the proposed Fishermen's Atlantic City Windfarm. The project originally proposed to deploy five turbines, each with a rated power of 5 megawatts (MW) and a 115-meter (m) rotor. The proposed plant layout is to have the turbines in a line with equal spacing of 1,008 m or 9.4 rotor diameters. High-fidelity computational fluid dynamics (CFD) were used to simulate the flow including the turbine wakes. Not only were wake effects on power production and aerodynamic loads (including fatigue loads) explored, but the idea of wake redirection through turbine yaw misalignment to decrease wake effects on power production was also explored.

The idea of wake redirection through yaw misalignment is based on the fact that in addition to torque, the turbine rotor creates a strong thrust force that opposes the flow (and that creates a wake). The thrust is normal to the rotor plane. If yaw misalignment is applied such that the rotor plane normal direction is no longer parallel to the flow, then the thrust now has one component in the flow direction and one perpendicular to it. The thrust force perpendicular to the flow creates an acceleration of the flow in the cross-stream direction, thus deflecting the flow and the wake. Wake redirection through yaw control is not a new idea. It has been explored through simulations at the National Renewable Energy Laboratory (NREL) by Fleming et al. [1,2] and elsewhere by Jiménez et al. [3]. The Energy Centre of the Netherlands (ECN), the third author's affiliation, holds a patent on the wake-redirection idea [4,5]. The Fishermen's Atlantic City Windfarm analysis conducted for this paper was the team's first experience with simulating wake redirection for a planned wind plant in the regulatory process with the intent to install instrumentation to validate the modeling results. Measurements collected at Fisherman's Atlantic City Windfarm will be used to quantify the accuracy of the high-fidelity wake analysis tools used in this work and to provide additional information on wind-plant-wake interactions and their influence on performance and mechanical loads.

Large-eddy simulation (LES) was used because it directly resolves the larger and important energy-containing scales of turbulence in the flow while modeling the remaining smaller scales. LES is the highest fidelity type of CFD available for performing wind plant simulations that remains computationally feasible; each simulation required 1,800 computational cores over a period of 60–70 hours (roughly 100,000–125,000 computer core-hours) to obtain 1,000 seconds of simulation data. LES is coupled with an actuator line representation of the turbine aerodynamics to create wakes.

A precursor atmospheric LES was first created to provide the turbulent atmospheric inflow. It was tuned to best match the average conditions for the wind sector of interest. Those precursor inflow data were saved and used as inflow for the wind plant simulation. All five turbines of the proposed wind plant were simulated. A case of particular interest is when winds are out of the southwest in which the wind is predominantly down the row of turbines creating strong wake effects on all but the most upstream turbine, a fairly common situation at the proposed site. Also of interest is when wind speeds are at or below the 12.5-meter/second (m/s) rated wind speed of the turbine (operation within Region 2 of the turbine) because that is where wake effects are strongest. Therefore, we simulated winds directly down the row and below rated speed to examine worst-case wake effects. Because the likelihood of the wind direction being aligned directly with the row is small, a wind direction offset from the row direction by a few degrees was also simulated.

The remainder of this document discusses the simulation method in more detail, shows the specific inflow conditions simulated, presents results of the simulations, and provides conclusions.

Simulation Method

As stated above, the simulation type used in this study is LES. There is a variety of types of CFD. At the highest fidelity is direct numerical simulation (DNS) in which all turbulent scales are directly resolved in time and space. In a wind plant, the smallest turbulent scales are on the order of a millimeter and the largest are on the order of a hundreds of meters or even kilometers. That means a computational domain that spans hundreds of meters or kilometers is necessary but with a grid resolution on the order of millimeters. A 1-kilometer (km) cube domain with 1-millimeter (mm) resolution would require 1×10^{18} grid cells, far beyond our current computing ability.

On the other end of the fidelity range is CFD based on the Reynolds-averaged Navier-Stokes (RANS) equation, which gives a time-averaged representation of the flow. Only the mean part of the flow is resolved, and the effect of turbulence is completely modeled. Because the turbulence is not explicitly resolved but rather its effect on the mean flow is modeled, the computational requirements are a fraction of that of DNS. The tradeoff, though, is that there is heavy reliance on a turbulence model, and turbulence is extremely complicated and difficult to model. There is no one turbulence model that works well in all the turbulent regimes seen in a wind plant.

LES lies in between RANS and DNS. It directly resolves the more important, larger scales of turbulence and models the effect of the remaining smaller scales. Because only part of the turbulence is being modeled and the part that is modeled is the smaller, more isotropic part, it is easier to accurately model, and errors in the turbulence modeling are not as pronounced as with RANS. In this case, we use the scale-independent Lagrangian-averaged dynamic Smagorinsky model of Meneveau et al. [6]. In the case of the proposed Fishermen's Atlantic City Windfarm, the domain spans several kilometers because the actual wind plant is proposed to be that large, but a variable-resolution computational grid is used that has roughly 8-m cells to capture the atmospheric turbulence and roughly 2-m cells to capture turbine wakes. This results in a grid containing roughly 1×10^8 cells, which is much more tractable than what would be required by DNS.

The LES strategy employed in this study is to first perform a precursor atmospheric simulation. That is, the atmospheric boundary layer flow is simulated in the absence of turbines using a horizontally periodic domain (in effect making an infinitely long domain). The effects of buoyancy caused by temperature gradients in the atmosphere are included, which is key to simulating different types of atmospheric stability and also the effects of the Earth's rotation through the Coriolis force. As the precursor simulation advances in time, the atmospheric boundary layer and its turbulence develops. At some point, the boundary layer comes to quasi-equilibrium, and velocity and temperature data at horizontal boundaries can be saved every time step over some duration. The saved data are then used as inflow to a separate wind plant simulation that includes the model for the turbines that creates wakes. In short, the simulation is a two-step strategy in which a precursor simulation is performed that creates inflow boundary condition data for the wind plant simulation.

The turbines are modeled as actuator lines [7], which is a fairly common strategy in wind plant LES. With the actuator line, the turbine rotor geometry is not explicitly modeled. To explicitly capture the rotor geometry requires a complex computational grid that conforms to the rotor shape and that contains very small cells to capture the boundary layer of the blade, making the problem too computationally expensive. The actuator line models the turbine blades as lines along which are distributed body forces that mimic the lift and drag forces distributed along the span of actual blades. The method samples the velocity along the actuator line. With the velocity information, the blade angle of attack along the blade is found. Airfoil look-up tables of coefficient of lift and drag versus angle of attack are used. Using the velocity and coefficient of lift and drag along the actuator line, actual lift and drag along the actuator line can be found. That force distribution is applied to the flow field, creating a low-speed wake and its turbulence-generating shear layer. The rotating actuator line representation of the rotor also allows us to examine how aerodynamic loads on the blades change in time. The fluctuating loads that contribute to fatigue damage can be extracted and the effect of wakes and wake redirection on power and loads can be examined.

Cases Simulated

The wind direction of interest is from the southwest in the direction of the five-turbine row of the proposed wind plant. The wind plant layout is shown in Figure 1, so the simulated wind is from the lower left to the upper right. In the worst-case scenario, the mean wind direction is straight down the row from 238.6°, creating direct waking. Because the probability of the wind being exactly aligned with the row is low compared to it being within a few degrees of exactly aligned, winds from 235° were also simulated; in this case, the downstream turbines are partially waked by the upstream turbines. It is also important to note that in examining the wind rose [8] in the site-assessment data, the wind is from the southwest a significant portion of the time. For a wind rose divided into twelve sectors of 30° width, there is a 12% probability of winds below the turbine's rated wind speed of 12.5 m/s coming from the southwestern sector from 225° to 255°.

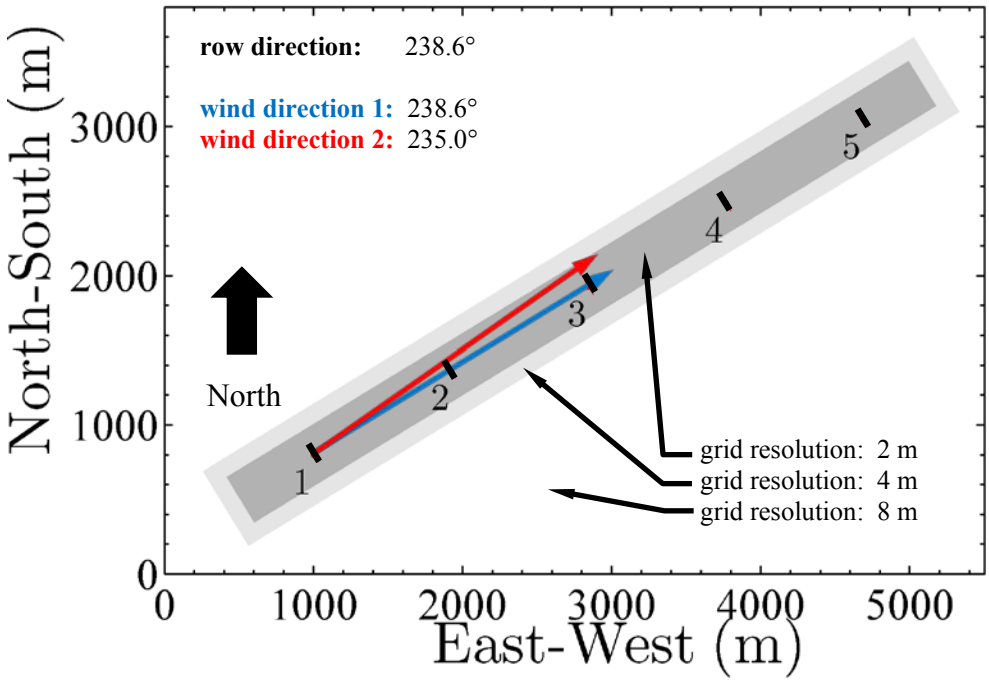

Figure 1: Wind plant layout. The numbered black bars are the turbines. The blue and red arrows show the simulated mean wind direction vectors. The regions of gray are those that have extra computational grid resolution to properly capture the turbulent structures in the turbine wakes.

In all cases (straight down the row or slightly offset), the mean wind speed is 9 m/s with a turbulence intensity of 5% and a shear exponent of 0.17. That 9 m/s speed was chosen because it is within the variable rotor speed region (Region 2) of the turbine's operating regime in which the rotor's thrust coefficient is maximum, which creates the strongest wake. This wind speed was also chosen because the 9 m/s wind speed bin taken from site-assessment data has among the highest of probabilities of occurrence in the southwestern wind direction sector. The turbulence intensity of 5% is slightly lower than the average for this wind speed and direction, but still within roughly one standard deviation of the mean value, so it is a condition that is regularly seen. The wind shear matches the mean wind shear for this wind speed and direction nearly exactly.

It is important to note that turbulence intensity and shear are not inputs into the precursor simulation, rather they are outputs. The simulation inputs are mean wind speed and direction at a certain height, surface roughness, surface temperature flux or heating/cooling rate, and the initial potential temperature profile (potential temperature is temperature with the effects of temperature change caused by expansion and compression of air parcels because of altitude change being removed). At this stage in the program our best judgment was used, based on past experience, to decide which combination of these inputs would yield a shear and turbulence intensity in good agreement with reality. To achieve the conditions simulated, a surface aerodynamic roughness height of 0.1 mm was used, which is

typical for flow over water [9]. The initial vertical potential temperature profile was to have a constant temperature of 285 kelvin (K) up to 350 m above the surface. Then, a capping inversion was applied in which the temperature increased by 5 K over the next 100 m. Above that strong inversion, the profile is slightly stable with an increase of 3 K per 1,000 m. The surface temperature is specified to cool by 0.25 K/hr. Although the ocean likely does not cool like this, winds coming from relatively warmer land and then flowing over relatively cooler land would see the same effect as flow over a homogeneous surface that cools in time. The simulation is run for 15,000 s of simulation time to reach quasi-equilibrium. In effect, slightly stable atmospheric conditions are produced.

The mean velocity profile of the precursor simulation for the 235° wind direction is shown in Figure 2, along with the mean potential temperature profile. The power law velocity profile for a shear exponent of 0.17 is shown as a red line and matches well with the actual profile. The capping inversion is clearly seen in the profile of potential temperature, and it is reflected in the velocity profile (i.e., the velocity is constant or geostrophic above that inversion).

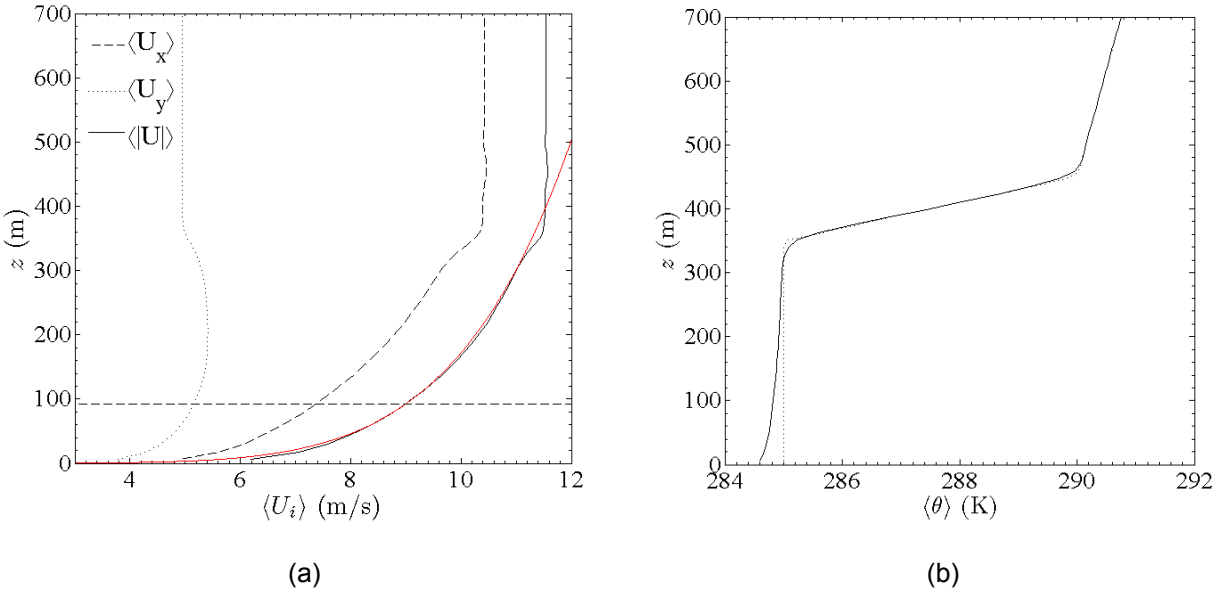

Figure 2: Mean velocity (a) and mean potential temperature (b) profiles from the precursor. In the velocity plot, the red line is the profile for a shear exponent of a 0.17, which matches the actual profile well and the dashed horizontal line denotes the turbine hub height. In the temperature plot, the dashed line denotes the initial profile. Both profiles are after 15,000 s of simulation time.

For the precursors (one for each wind direction), a domain of 5.5 km × 3.8 km × 1 km in the east-west, north-south, and vertical directions, respectively, is used with a uniform resolution of 12 m. For the wind plant simulations, the same domain size is used, but the background resolution is uniformly 8 m. Then there are regions of successive refinement around the turbines and their wakes in which the resolution increases to 2 m. That higher, finest resolution is required to capture the important scales in the wakes, which are smaller than the important ones in the atmosphere. Also, this local refinement keeps the problem size tractable; had a 2-m resolution been used throughout the domain, the domain size would have been 20 times larger than its size of 1.14×10^8 grid cells, which would have cost at least 20 times more computationally. The successive refinement regions are shown in Figure 1.

The original turbine proposed for Fishermen's Atlantic City Windfarm was modeled, and it has a 115-m rotor diameter and a 5-MW rated power generation that occurs at roughly 13 m/s. At the 9-m/s mean wind speed simulated here, the nominal power curve indicates that the turbine produces 1.87 MW. Turbine operating curves, blade profiles, and airfoil look-up tables were provided by the manufacturer.

Results

The results section is divided into two parts: first, the results for wind aligned exactly with the row direction are discussed, and second, the results for wind direction offset from the row direction are discussed. These sections are then followed by general discussion. In this section, when mean quantities are discussed, we are referring to time-averaged. The simulation duration is 1,000 s, and the averaging is over the final 800 s because the first 200 s contains the transient in which wakes form and are propagated downstream.

Mean Wind Aligned with the Row.

Four cases for the wind aligned exactly with the row were simulated. In the baseline case, no wake redirection was applied, so the yaw misalignment of all turbines is 0°. In the other cases, we examined yaw misalignments of 15°, 20°, and 25° on the first four turbines in the row. The fifth turbine does not require yaw misalignment because it does not wake another turbine, so its wake need not be deflected. Figure 3 and Figure 4 show cross sections of instantaneous and time-averaged velocity, respectively, for both the baseline and the 25° yaw misalignment cases. Both cases are shown side by side for ease of comparison, but were simulated separately. The wakes are clearly visible, and the deflection for the 25° yaw misalignment case is clearly visible. The meandering nature of the instantaneous wake is easily observed in Figure 3. Figure 4 shows the mean wake velocity. In Figure 5, we also show the z-component of vorticity, which indicates rotation in the flow about the vertical axis. Rotation exists in regions of high shear, such as the shear layer at the edges of the wake, where we see most of the vorticity. Positive vorticity indicates counter-clockwise rotation in the flow.

The wakes were redirected to the southeast rather than the northwest for two reasons. First, for an unwaked turbine with no yaw misalignment, a rotor blade experiences an out-of-plane (OOP) blade-root bending moment that is cyclic with a period equal to the rotor rotation rate. This behavior is caused by the fact that there is vertical atmospheric shear so the blade experiences faster oncoming flow when it is pointed up than when it is pointed down, causing the periodic force. The same occurs for a rotor subject to non-sheared flow but with yaw misalignment. When a blade is horizontal but moving upward, the angle of attack of the blade is different than when it is on the other side of the rotor disk and horizontal but moving downward, causing different forces. Interestingly, the combination of sheared inflow and yaw misalignment can cause a cancellation of the force imbalances, leading to decreased amplitude of the cyclic loading (i.e., weaker fatigue loading). Second, the wakes were redirected to the southeast rather than the northwest because of the asymmetric nature of the wakes. Because the flow applies a torque to the rotor, the rotor applies an equal and opposite torque to the flow, causing the wake to rotate counter to the rotor rotation sense. The Darwind turbines' rotors rotate clockwise as viewed from upstream, so the wake rotates counterclockwise. Because of atmospheric shear in which the winds above have higher speed than the winds below, the wake rotation brings slower-moving air from below up to the right side of the wake as viewed from upstream. The wake rotation also brings faster-moving air down to the left side of the wake as viewed from upstream. This behavior is clearly visible in Figure 6, in which we see slower flow on the southeast side of the wake. It is better to subject the next turbine to the more energetic part of the wake (the northeast side), so we redirect the wakes to the southwest.

In terms of power production, having the mean wind aligned exactly with the rows, as shown in this set of results, is the worst case scenario. For the baseline case, under these conditions, the wind plant operates with an efficiency of 59.7%, with efficiency defined as the sum of the time-averaged power production of all five turbines divided by five times the time-averaged power of the unwaked turbine 1. The time history of the power of all five turbines for the baseline case is shown in Figure 7. Clearly, turbine 1 produces much more power than the other turbines.

It must be noted that in reality, the mean wind direction would most likely not remain exactly locked on the row-aligned direction, which would raise this efficiency value. Also, efficiencies as calculated by empirical models used by wind plant planners are given for a certain direction sector, often with a width of at least 10°, and averaged over a wide sector that predominantly includes partial waking rather than worst-case direct waking, which will significantly increase the efficiency value. Furthermore, such efficiency calculations take into account all wind speeds and their probability distribution; for winds above rated, the plant efficiency increases and, at some point before cut-out speed, reaches 100%. In this case, we only considered a single wind direction, not a sector, and one wind condition, which provides the worst-case value.

Figure 8(a) shows the effect of applying wake redirection through yaw misalignment. As the yaw misalignment is increased, the efficiency of the plant increases. The efficiency is 8% higher when yaw misalignment of turbines 1–4 is 25° than for the baseline case. It appears that a fraction of a percent more efficiency could be gained with even more yaw misalignment.

Figure 8(b) shows the percentage increase or decrease in efficiency of each individual turbine under wake-redirection control relative to the same turbine for the baseline case. The unwaked turbine 1 experiences a decrease in efficiency because yaw misalignment effectively reduces the inflow wind speed and surface area of the rotor. Larger yaw angles cause larger efficiency reductions. On the other hand, turbines 2–5, experience an increase in efficiency. This net increase is the sum of a larger increase because of reduced wake effects and a decrease because of yaw misalignment. This efficiency increase is especially true of turbine 5, which is never misaligned, so it does not experience the efficiency reduction caused by misalignment.

The increase in power production efficiency of the wind plant caused by wake redirection does not come without a penalty. Yaw misalignment causes changes in fatigue loads on the turbines. Figure 9 shows the time history of out of plane (OOP) blade-root bending moment over a roughly 20 s period of time. Over this time, the rotor makes roughly four complete rotations.

To quantify changes in fatigue loads, we must study the load fluctuations. First, there is a low frequency variation in OOP blade-root bending moment caused by changes in wind speed because of large-scale turbulence in the wind and turbine wakes. Second, there is a rotor rotation frequency caused by once-per-revolution passage of the blade through wakes or atmospheric shear. We are concerned with this rotor rotation frequency component of the fatigue load, so finding the fluctuation about a running mean that filters out the higher frequency part of the time history is appropriate. The root mean square (RMS) of this fluctuation time history is taken to obtain a global measure of fatigue loading.

Figure 10 shows how OOP blade-root bending moment RMS values change because of wake redirection. Figure 10(a) shows how the OOP blade-root bending moment RMS values increase in turbines 2–5 relative to the turbine 1 in the baseline case. Interestingly, for the baseline case, turbines 2–5 see a slight decrease in fatigue loads, possibly because the direct waking subjects these turbines to lower wind speeds and decreased atmospheric shear caused by turbulent mixing from the wake. However, when wake redirection is applied, the RMS loads increase on turbines 2–5. This is more clearly seen in Figure 10(b), which compares the loads of each turbine in the yawed case to the loads of the corresponding turbine in the unyawed case. As discussed earlier, the direction of yaw misalignment causes a cyclic OOP blade-root bending moment that cancels with that caused by atmospheric shear, so turbine 1 experiences a load reduction. Turbines 2–5 experience RMS load increases because they have transitioned from being fully waked, in which a blade experiences fairly homogeneous flow through an entire revolution, to being partially waked in which a blade passes in and out of a wake in a revolution. The velocity in the wake is much different than out of the wake, causing an increase in the amplitude of the cyclic loading.

The fact that loads increase when wake redirection is used to increase power capture can be mitigated using individual blade pitch control (IPC) layered on top of yaw misalignment. IPC applies a sinusoidal variation to the blade pitch as a function of blade azimuth angle. Therefore, a more constant blade loading can be obtained with IPC than with the standard collective pitch control. Prior work in this area [2] conducted at NREL shows that IPC layered on top of yaw misalignment can greatly mitigate the increased fatigue loading caused by yaw misalignment with little or no reduction in power capture.

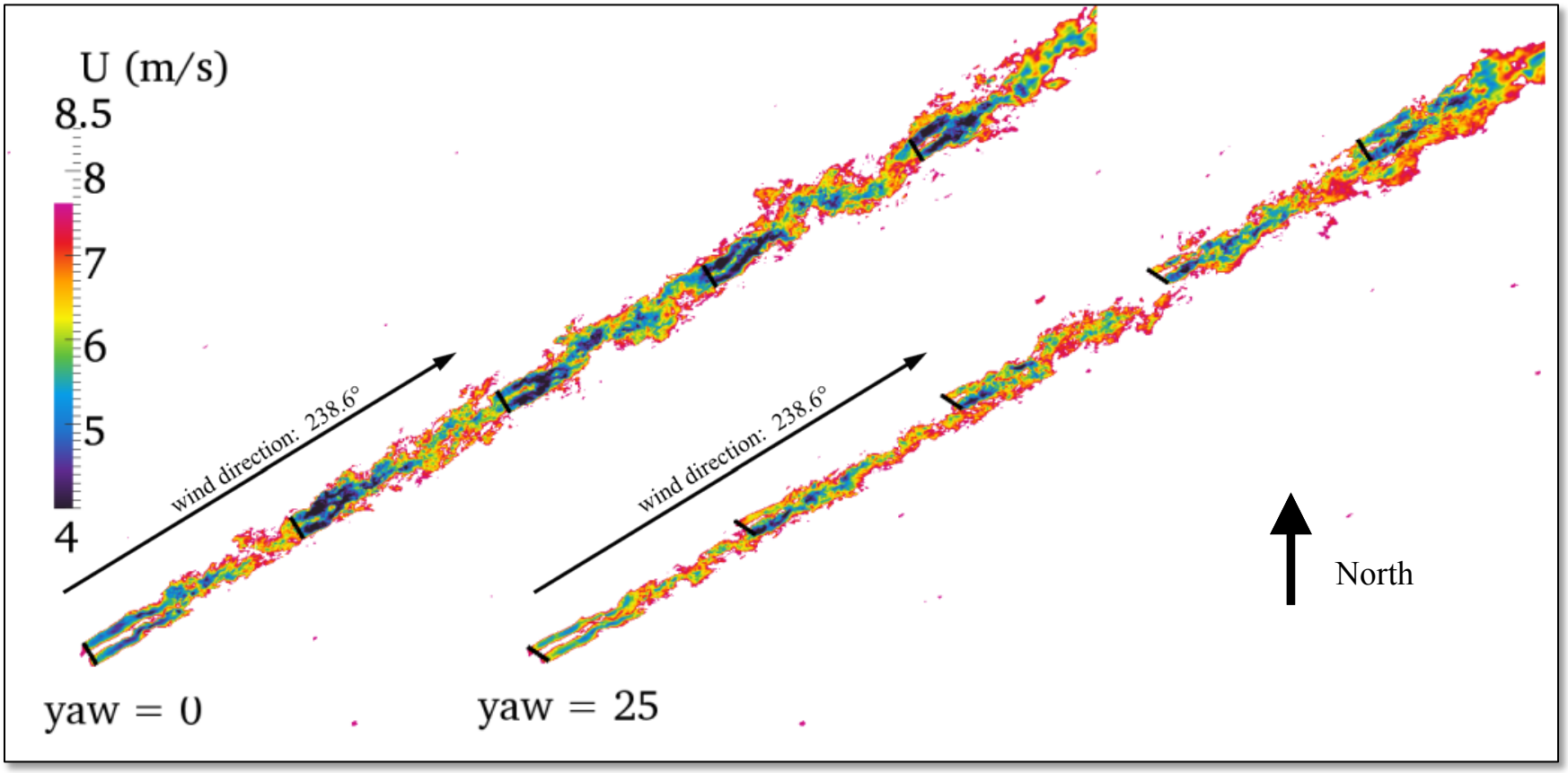

Figure 3: Horizontal contour planes of instantaneous velocity at hub height from simulations with the wind direction aligned exactly with the row direction. Both the 0° and the 25° yaw misalignment cases are shown side by side for comparison, although they were simulated separately. The turbine rotors and their orientations are shown as black lines.

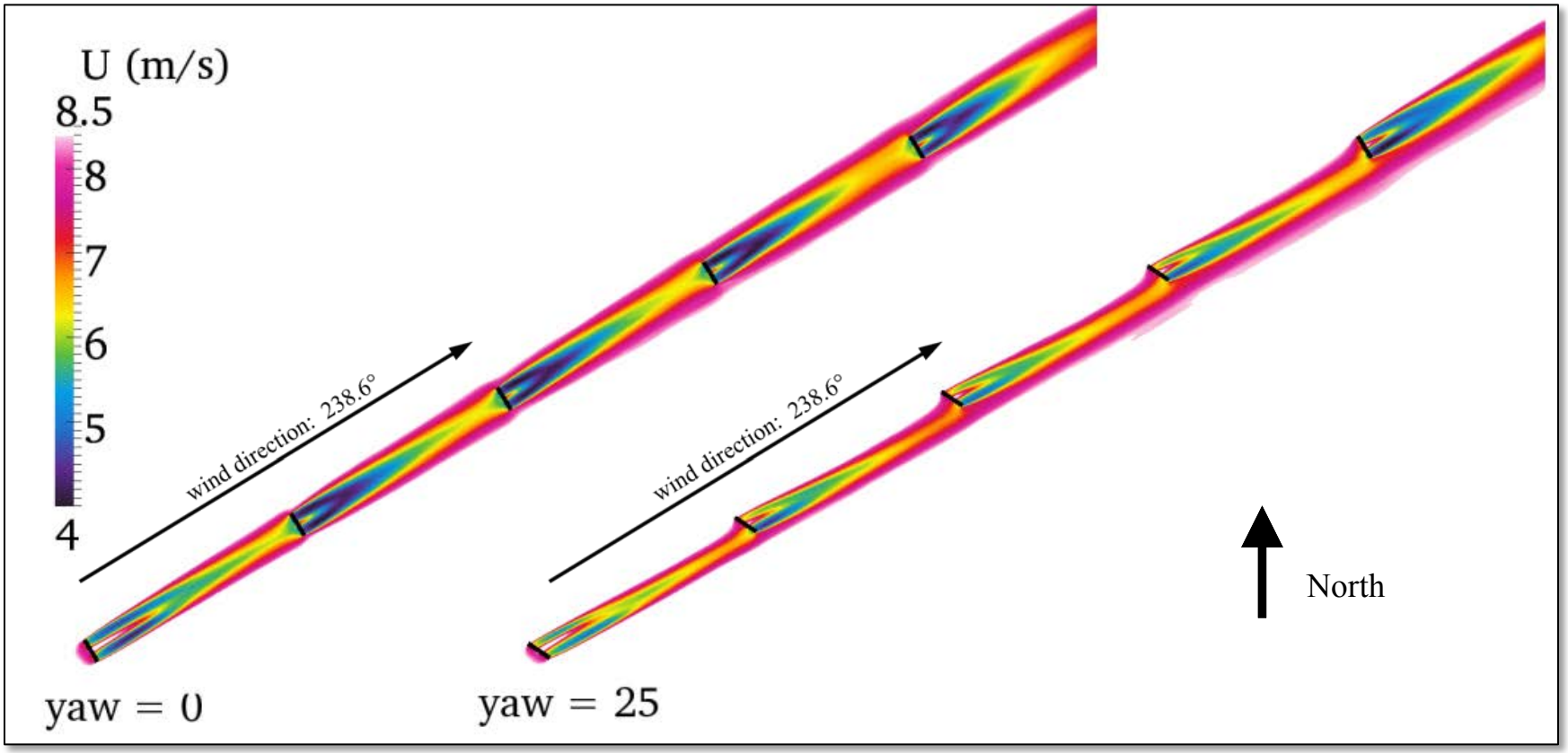

Figure 4: Horizontal contour planes of mean velocity at hub height from simulations with the wind direction aligned exactly with the row direction. Both the 0° and the 25° yaw misalignment cases are shown side by side for comparison, although they were simulated separately. The turbine rotors and their orientations are shown as black lines.

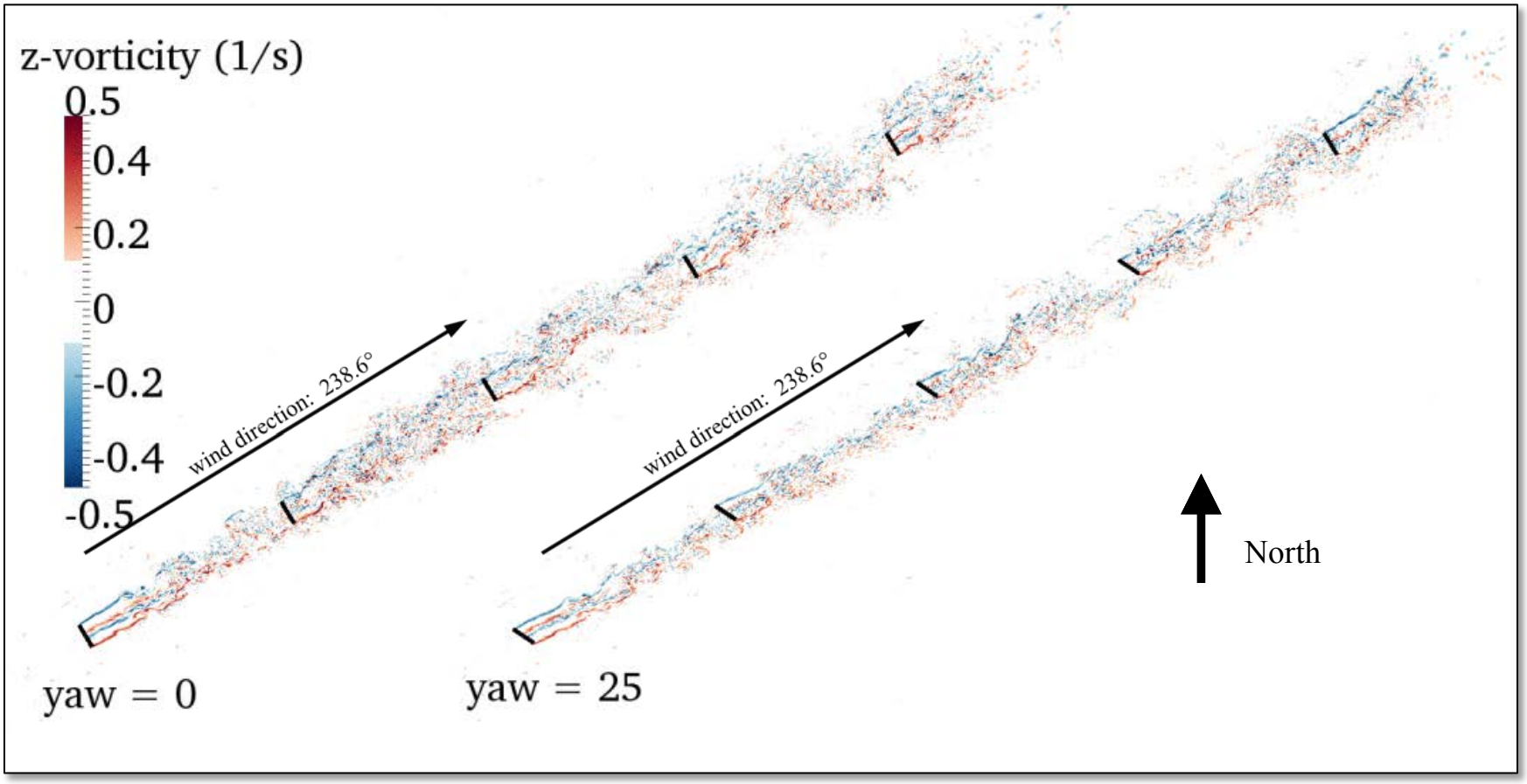

Figure 5: Horizontal contour planes of instantaneous vorticity at hub height from simulations with the wind direction aligned exactly with the row direction. Both the 0° and the 25° yaw misalignment cases are shown side by side for comparison, although they were simulated separately. The turbine rotors and their orientations are shown as black lines.

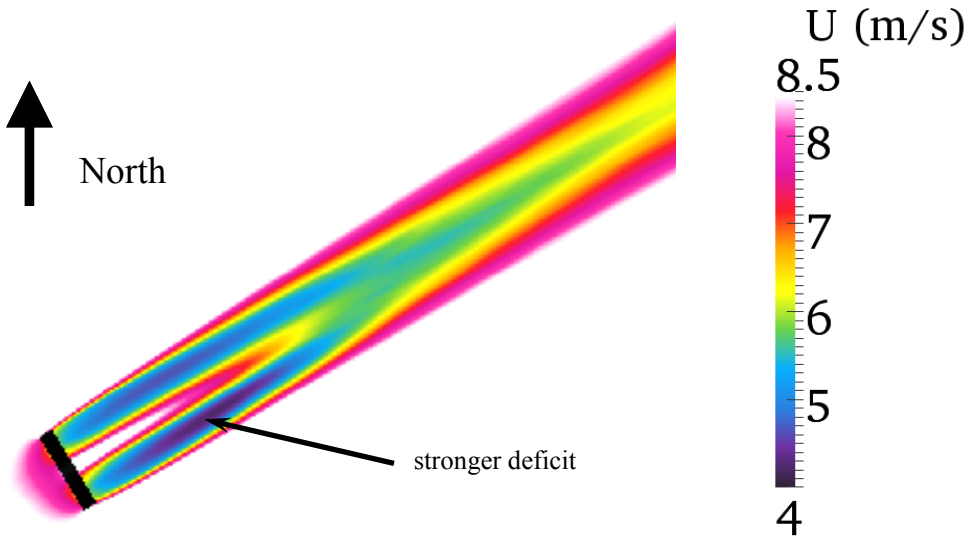

Figure 6: A close-up view of the mean contours of velocity in a horizontal plane at hub height. The wake deficit is stronger (lower velocity) on the southeast side of the wake, so redirection to the southeast is beneficial.

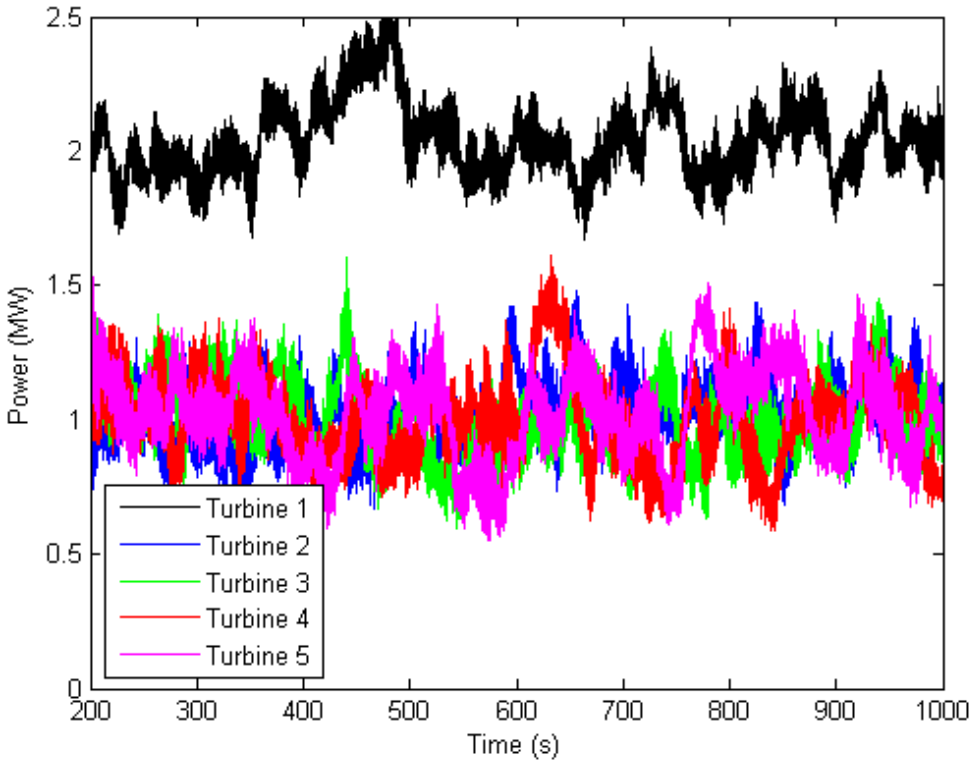

Figure 7: A time history of power production of all five turbines for the baseline case with mean hub-height wind direction aligned exactly with the row direction.

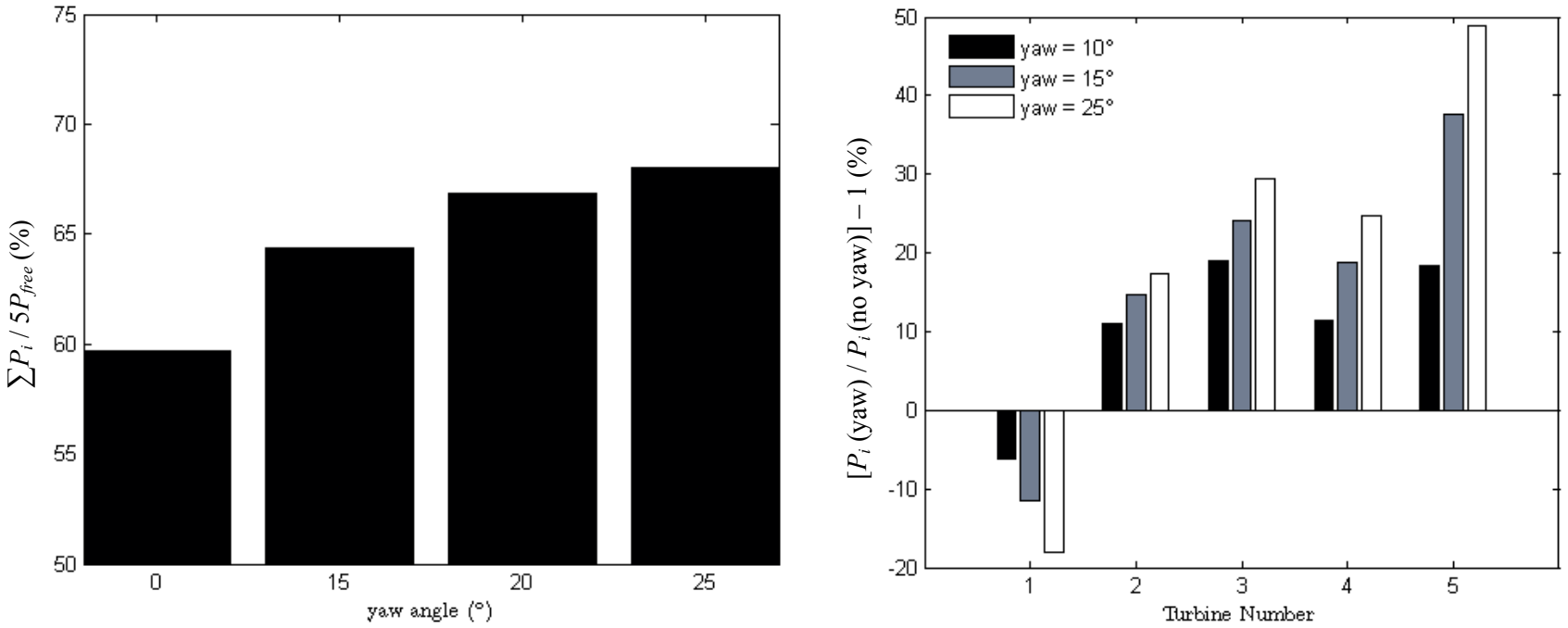

(a) (b)

Figure 8: (a) Efficiency of the wind plant for different levels of wake redirection through yaw misalignment; (b) increase/decrease in efficiency of each turbine under wake-redirection control relative to the corresponding turbine in the baseline, no-control case. These results are for the cases in which mean wind direction is aligned exactly with the row direction.

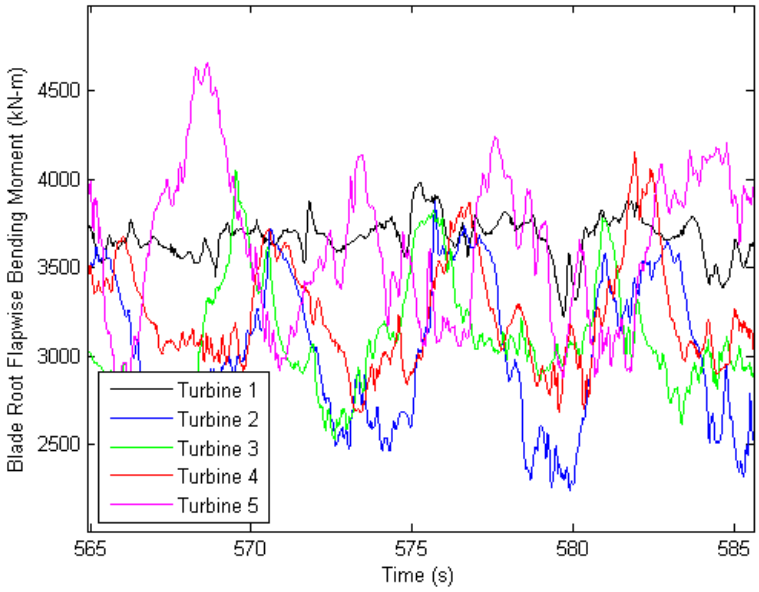

Figure 9: A time history of the OOP blade-root bending moment.

Mean Wind Offset from the Row.

This section is arranged very similarly to the previous one, but here we present results for the cases in which the mean wind is offset from the row direction by a few degrees are presented. Here the wind direction is 235° and the row direction is 238.6°. The wind speed, turbulence intensity, and shear are the same as in the row-aligned wind case. This case was examined because the row-aligned mean wind case will occur very seldom. More commonly under waked conditions, the wind direction will be offset from the row a few degrees. In this case, with no wake redirection, each waked turbine experiences roughly half the wake of the next upwind turbine. A baseline case with no yaw misalignment and also wake-redirection cases with yaw misalignment of 10° and 15° were simulated. Also, because the wakes convect to the northwest of each subsequent turbine under baseline conditions, when wake redirection was applied, the wakes were redirected further to the northwest. In the previous section for winds aligned with the row, we redirected the wakes to the southeast for reasons discussed there.

The instantaneous and mean contours of velocity in a horizontal plane at hub height for these cases are shown in Figure 11 and Figure 12, respectively. As in the previous section, each case is simulated separately but shown here side by side for ease of comparison.

Figure 13 shows the power production efficiency of the wind plant for the baseline and wake-redirection cases. Figure 13(a) shows the cumulative power of the wind plant divided by the power produced by five unwaked turbines (five times the average power of the unyawed turbine 1). With no wake-redirection, the plant efficiency for this wind direction and condition is 80%, but by using a 15° yaw misalignment the efficiency is increased to 90%. Figure 13(b) shows the percent increase in average power produced by each turbine in the wake-redirection cases relative to the corresponding turbine in the no-redirection case. Yaw misalignment causes a reduction in power capture, but the benefit of moving the wake outweighs that reduction. The yaw misalignment of turbine 1 causes a decrease in its power, but turbines 2–5 all increase in power because of mitigated wake effects. The increase in power of turbine 5 for the yawed cases is greatest because that turbine is not yawed (so it does not have the decrease in power caused by yaw misalignment), but it still benefits from the decreased waking from turbine 4.

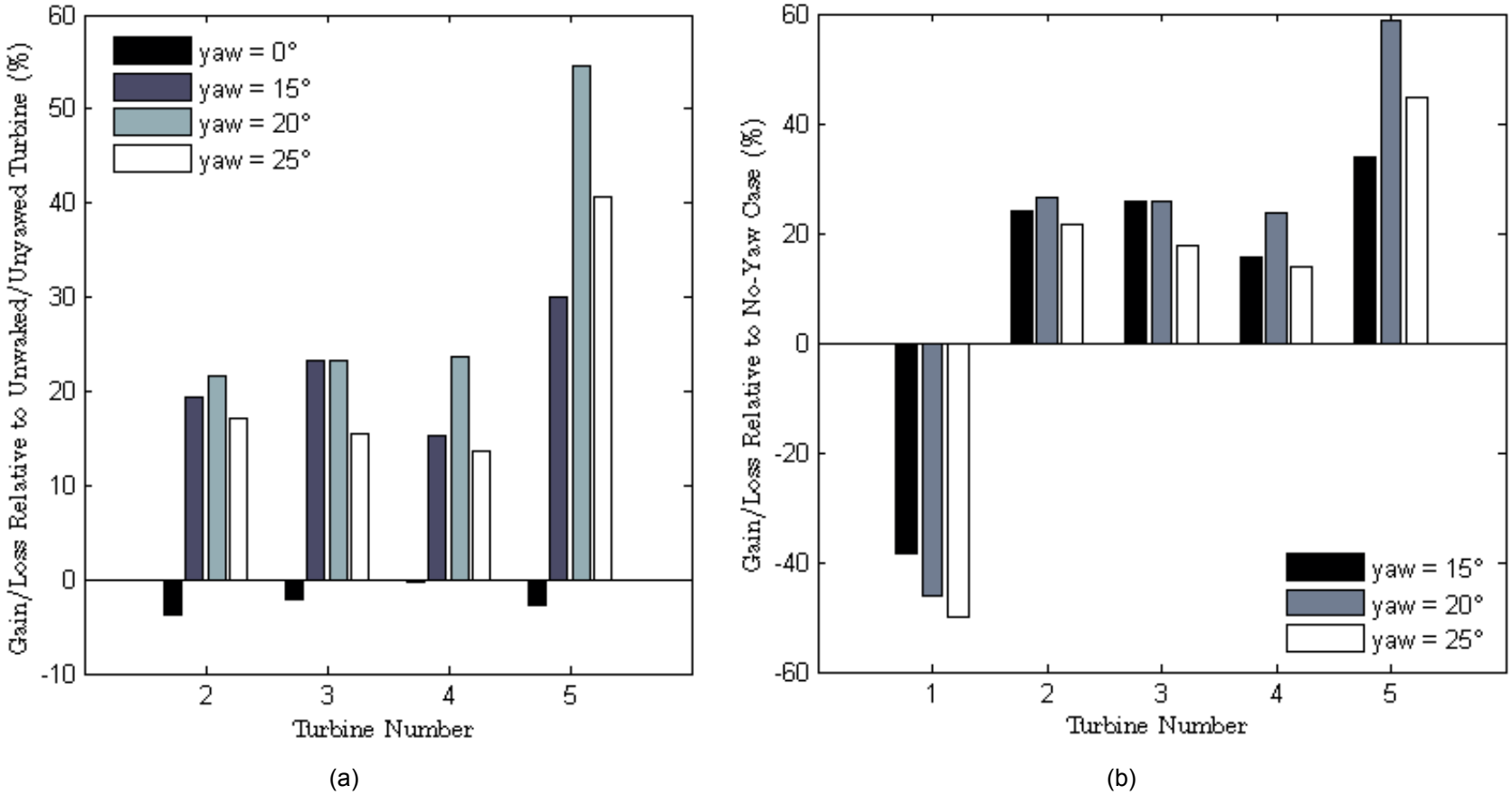

Figure 10: (a) Increase/decrease in OOP blade-root bending moment RMS value of each turbine relative to the unwaked turbine 1 in the baseline no-control case. (b) Increase/decrease in OOP blade-root bending moment RMS values of each turbine under wake-redirection control relative to the same turbine in the baseline no-control case. These results are for the cases in which mean wind direction is aligned exactly with the row direction.

Figure 14 shows how OOP blade-root bending moment RMS loads change because of wake redirection. Figure 14(a) shows how these RMS loads increase in turbines 2–5 relative to turbine 1 in the unyawed case (lowest fatigue load turbine and case). Even for the unyawed case, turbines 2–5 see increased fatigue loads from partial waking, and the blades periodically pass through the low-speed wakes causing load fluctuation. However, when applying wake redirection, the RMS loads increase on turbines 2–4, but decrease on turbine 5. This is more clearly seen in Figure 14(b), which compares loads of each turbine in the yawed cases to the loads of the corresponding turbine in the unyawed case. In the wake-redirection cases, turbines 1–4 are yawed, so yaw misalignment causes load increases. Turbine 5 is always unyawed, so it experiences no RMS load increase from yaw misalignment. Because the wakes of turbines 1–4 are redirected and do not impact turbine 5 as much as without redirection, a further RMS load reduction is seen.

In the previous section that discusses the wind aligned exactly with the row, turbine 1 experienced a decrease in loads because of yaw misalignment, which is caused by a cancellation in vertical wind shear-induced cyclic loads by yaw misalignment-induced cyclic loads. Depending on rotor rotation sense, this reduction occurs only for yaw misalignment in one direction. For yaw misalignment in the other direction, an increase in loads should occur, which we observe here. As explained earlier, though, the loads increase can be mitigated using using IPC layered on top of the yaw misalignment.

Effect on Overall Plant Performance.
Based on the findings in the previous two subsections, we fit a function to our data points of average wind plant power production (at 9 m/s with the 5% turbulence intensity and 0.17 shear exponent) versus wind direction with and without wake-redirection control. For each case of control and no control, there are three data points. There is power for the 238.6° (row aligned) and 235° directions, plus it was assumed that a direction, such as 210° for which wake effects are not a factor, has a power equal to five times the power of the unwaked, wind-aligned turbine. We assume the function is double Gaussian with minima at 238.6° and 121.4°, the two row-aligned wind directions. It is assumed that wake redirection would be equally effective for both row-aligned wind directions.

The Gaussian fit to the data is shown in Figure 15 for both the cases with and without wake-redirection control. The probability distribution of wind in the 8.5 m/s to 9.5 m/s bin as a function of wind direction was convolved with the Gaussian wind plant power production versus wind direction curve to obtain a plant efficiency over the wind rose. We stress the point that this calculation was only performed for the 9 m/s wind speed. As the wind speed exceeds the rated power, wake effects become negligible, but we do not have data points to show us at what wind speed that occurs. Also, there are no data points for different turbulence intensities and shear levels. Therefore, we are only comparing the wind plant efficiency over the entire wind rose with and without wake-redirection control for the 9 m/s case with the 5% turbulence intensity and 0.17 shear exponent.

Under these conditions for this site with no wake-redirection control, we predict that the wind plant is 94.2% efficient over a long duration in which winds will come from all directions. With wake-redirection control, the efficiency is improved 1.5%. Although seemingly small, a greater than 1% increase in efficiency is significant in terms of revenue over the 20-year lifetime of a wind plant. Over the entire wind speed distribution, this efficiency gain is expected to be smaller, though, because some of the time the turbines will operate in above rated wind conditions in which wake redirection is less effective. However, for the directions in which wake effects are important, there is significantly more probability that the wind speed will be under rated conditions in which wake redirection is most effective. Although the overall efficiency gain is modest, the gain would be more substantial in a full wind plant composed of more than one row in which there are more than two significant waking directions.

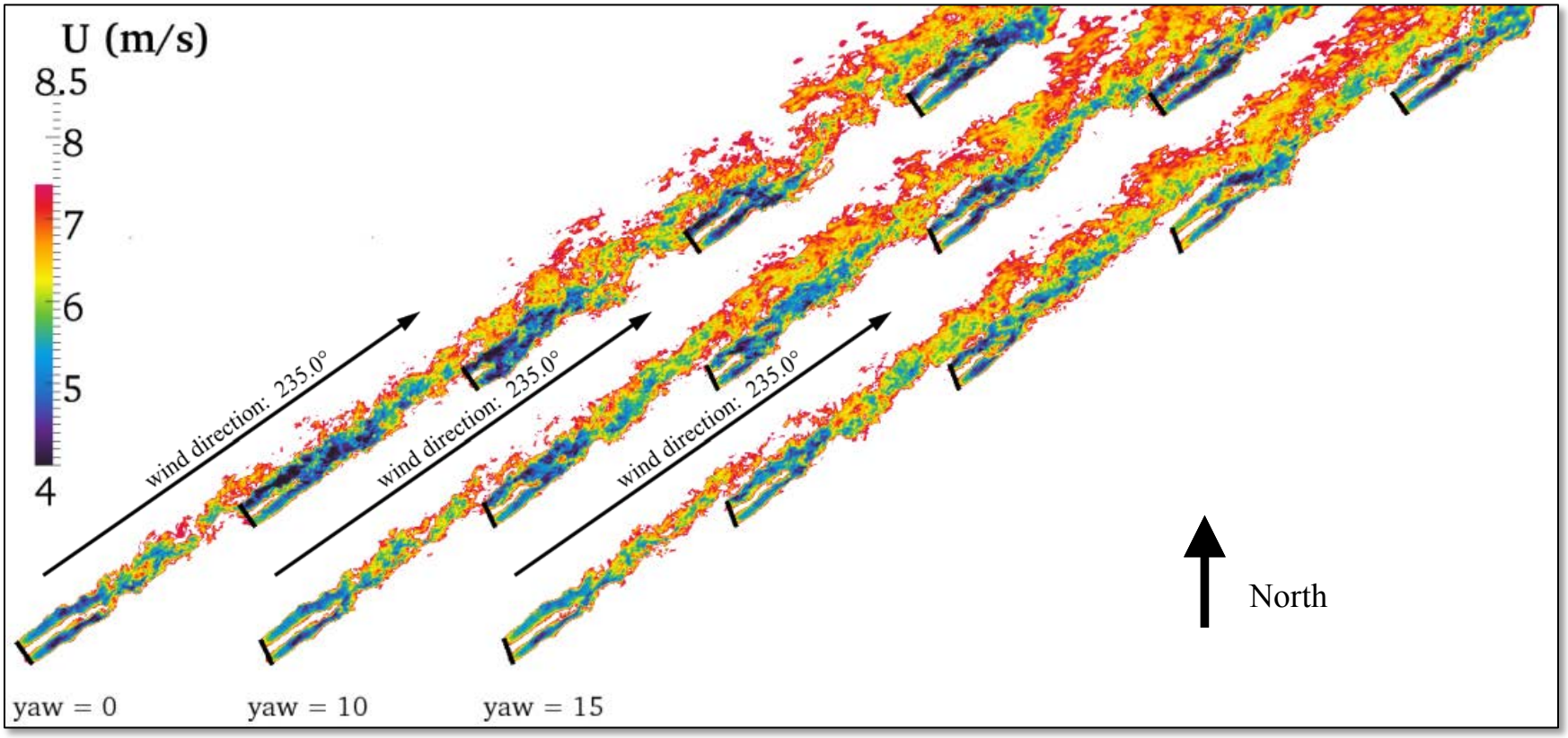

Figure 11: Horizontal contour planes of instantaneous velocity at hub height from simulations with the wind direction offset from the row direction. The 0°, 10°, and 15° yaw misalignment cases are shown side by side for comparison although they were simulated separately. The turbine rotors and their orientations are shown as black lines.

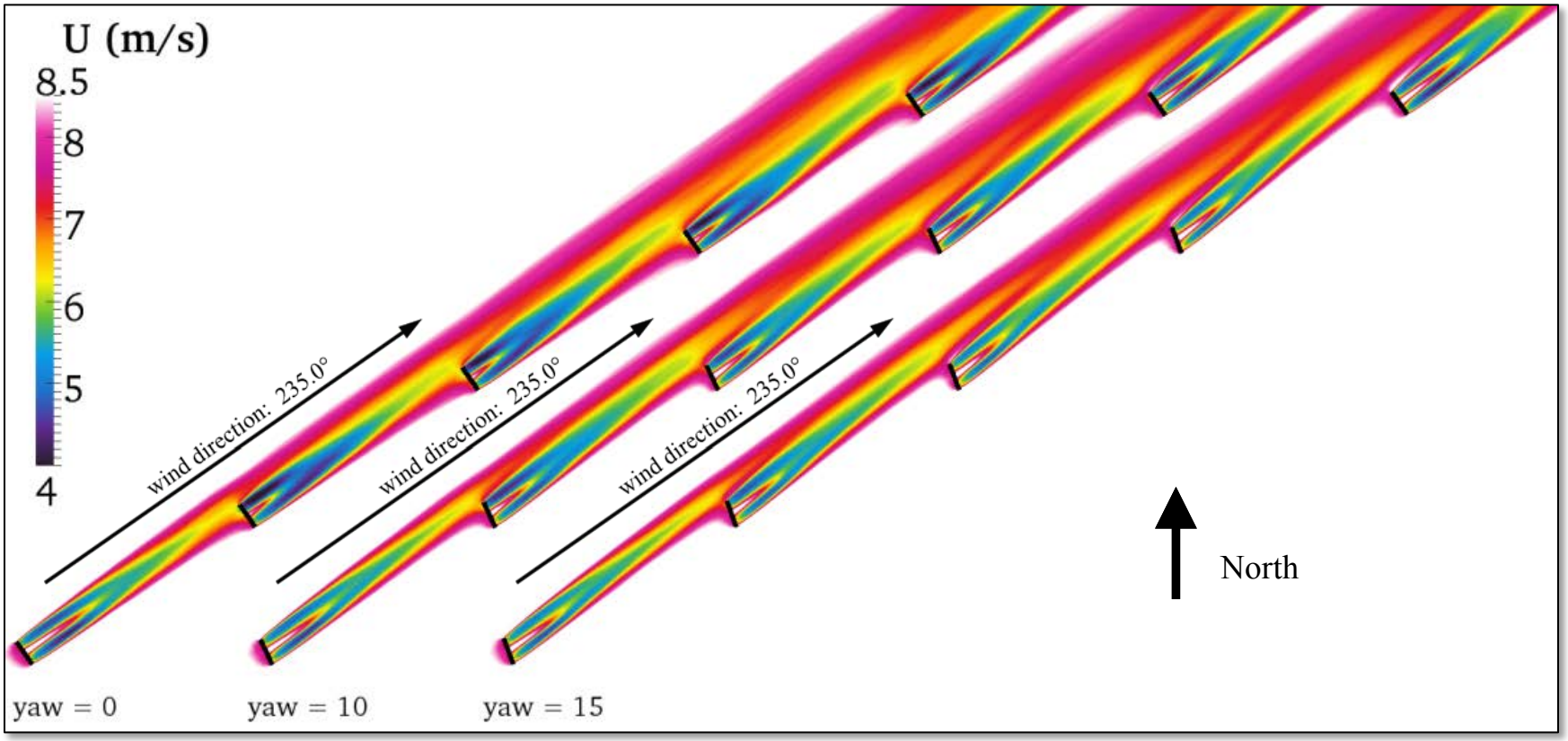

Figure 12: Horizontal contour planes of mean velocity at hub height from simulations with the wind direction offset from the row direction. The 0°, 10°, and 15° yaw misalignment cases are shown side by side for comparison although they were simulated separately. The turbine rotors and their orientations are shown as black lines.

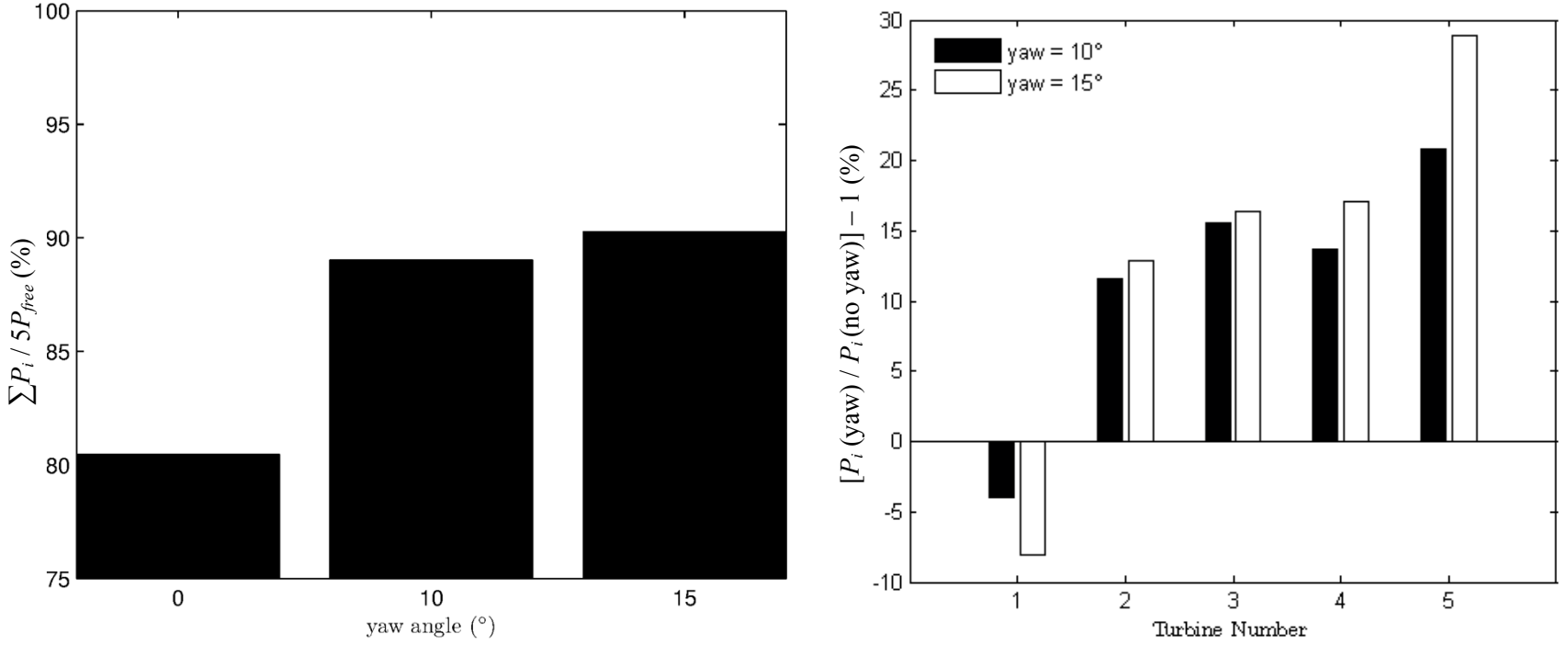

Figure 13: (a) Efficiency of the wind plant for different levels of wake redirection through yaw misalignment; (b) increase/decrease in efficiency of each turbine under wake-redirection control relative to the corresponding turbine in the baseline, no-control case. These results are for the cases in which mean wind direction is offset from the row direction.

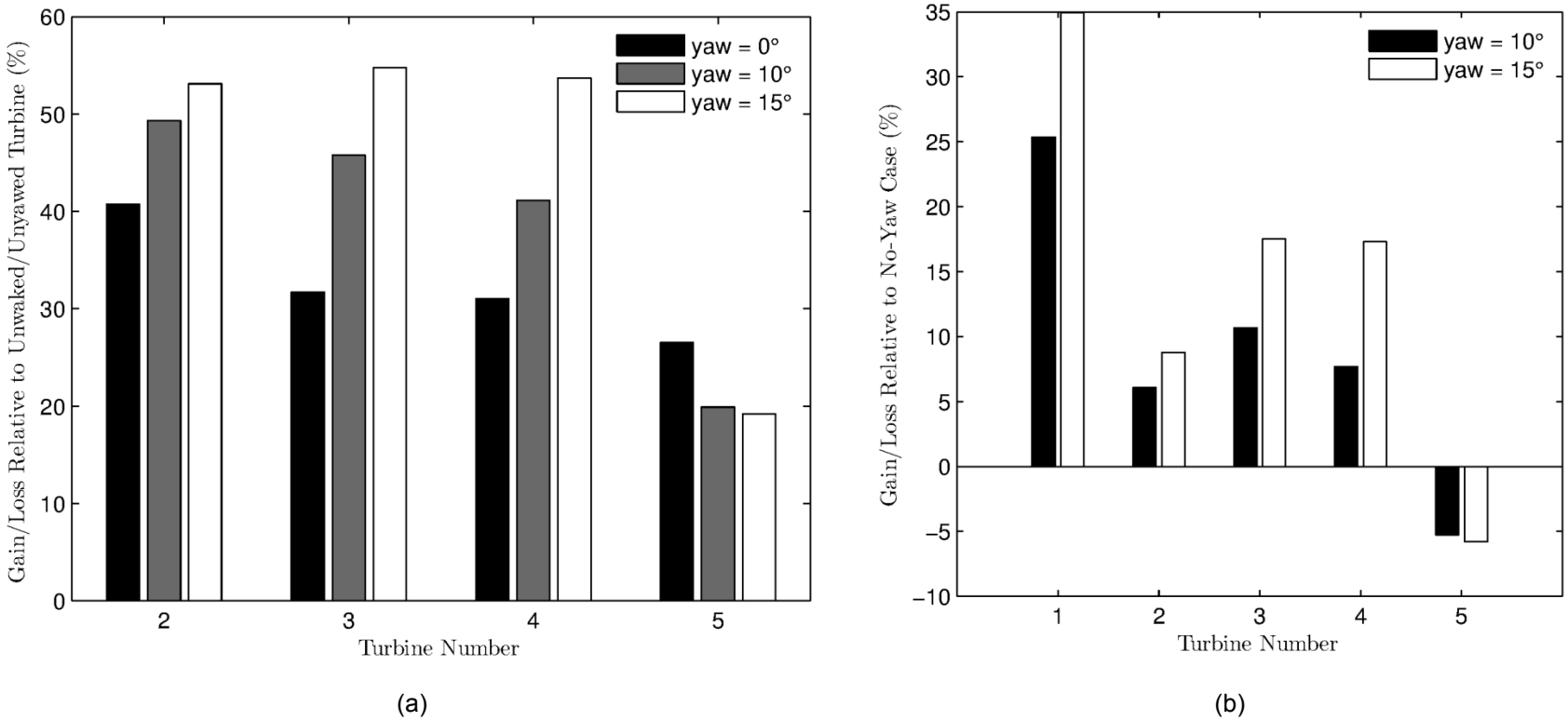

Figure 14: (a) Increase/decrease in the OOP blade-root bending moment RMS value of each turbine relative to the unwaked turbine 1 in the baseline no-control case; (b) increase/decrease in the OOP blade-root bending moment RMS values of each turbine under wake-redirection control relative to the same turbine in the baseline no-control case. These results are for the cases in which mean wind direction is offset from the row direction.

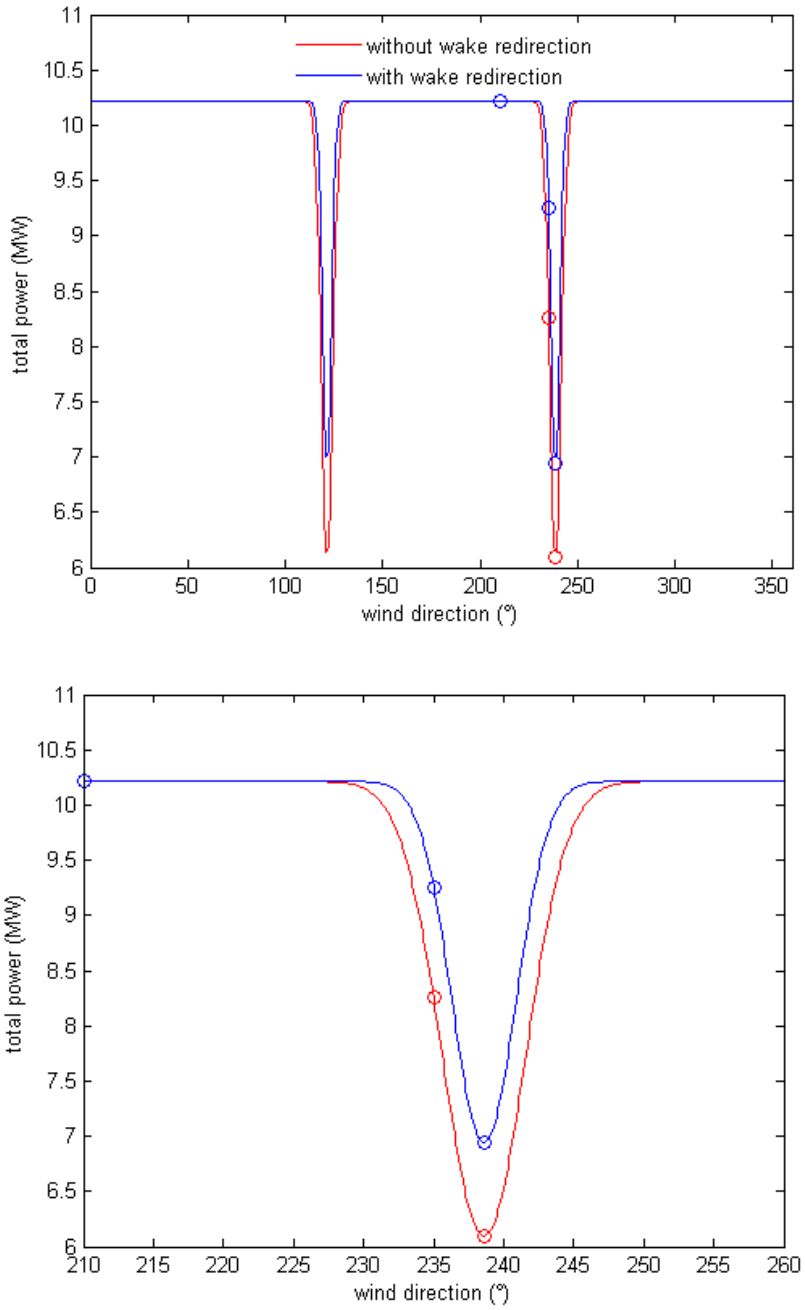

Figure 15: The double-Gaussian fit of total wind-plant power production versus wind direction for a wind speed of 9 m/s, a turbulence intensity of 5%, and a shear exponent of 0.17. The right-hand figure is the same as the left-hand figure, except the horizontal axis focuses on the 210°– 260° wind direction sector.

Conclusions

We performed preliminary high-fidelity large-eddy simulations of the flow through the proposed Fishermen's Atlantic City Windfarm. The turbines proposed for the project each have a rated power of 5 MW and a 115-m rotor. The five turbines in the plant are arranged in a line with equal spacing of 1,008 m or 9.4 rotor diameters. The focus of this study has been on winds out of the southwest, a direction sector for which there is a significant 12% probability of winds (based on field observations using 30° sectors) in which wake effects are important. Two main cases were examined: mean wind at hub height aligned exactly with the row direction and mean wind offset from the row direction by 3.6°. For both cases, the mean hub height wind speed, turbulence intensity, and shear were the same with values of 9 m/s, 15%, and 0.17, respectively. These values were chosen because they are representative of winds out of the southwest, and the 9 m/s wind speed is a speed in which the turbine is producing the maximum thrust coefficient and thus maximum wake effects.

For each of the two cases, a baseline simulation is performed with normal control strategies employed along with a series of simulations in which wake-redirection control was enabled through yaw misalignment of the turbines that wake other turbines (i.e., turbines 1–4). Turbine 5 has no yaw misalignment because it does not impact any other turbines with its wake. The idea of wake redirection is to steer the low-energy wake away from downwind turbines as much as possible to increase collective power production. Yaw misalignment, which pushes wakes to the side, lowers energy capture of the misaligned turbine, but the increase in power production in the remaining turbines because of reduced wake effects causes a net increase in production. For the wind aligned with the row and offset from the row, we observed increases in plant efficiency of 8% and 10%, respectively. The increases required yaw misalignment in the neighborhood of 20°.

The increase in efficiency comes with an overall increase in mechanical fatigue loads. This, in part, is caused by the yaw misalignment (however, as is shown in Section 4.1 of this report, if the yaw misalignment is in the right direction, a decrease in loads of the unwaked turbine can be experienced), and also by transitioning from the full wake to partial wake situation for the wind aligned with the row case. This should not be seen as an unsurmountable problem. If IPC were layered on top of the wake-redirection control, we believe, based on prior work, that the additional fatigue loading can be cancelled out.

The 8%–10% efficiency gain observed in these simulations is only for the two wind directions and conditions we studied for the Fishermen's Atlantic City Windfarm project, not for the entire wind rose or range of atmospheric conditions (i.e., turbulence intensity). The gain in annual energy production for the Fishermen's Atlantic City Windfarm would be more modest because there is significant probability of wind directions in which wake effects are not a factor. Although the gain in annual energy production would be modest for this wind plant, we predict that it may be in excess of 1%, which creates a sizable increase in revenue over the 20-year wind plant lifetime. Also, the gain in annual energy production would be more significant for a full wind plant with many rows such that there are many wind directions in which waking occurs.

Another important point is that the spacing at the proposed wind plant is 9.4 rotor diameters, which is quite large (for example, in comparison to the Horns Rev offshore wind plant in Denmark, which has 7-diameter spacing, or the Lillgrund wind plant in Sweden, which has 4.4-diameter spacing). We hypothesize that wake-redirection control would be more effective for closer turbine spacing because at closer spacing, the wakes have not diffused as much (i.e., they are narrower) and they have a stronger deficit. The effect of wake redirection on a turbine waked by a stronger, more concentrated wake should be more dramatic. We believe that the benefits of wake-redirection control would allow a wind plant developer to either 1) pack more turbines into a given watersheet area and increase total power output, or 2) achieve the same total power output on a smaller watersheet area. In the first case, more revenue will be generated; in the second case, the same revenue will be generated but with lower land lease or purchase cost as well as cabling cost (inter array and export).

The proposed wind plant provides a great opportunity to validate high-fidelity simulation tools like that used here and to fully explore wake redirection with highly instrumented turbines. In this work, we simply tried different yaw misalignment angles, setting the first four turbines of the row to an equal misalignment angle, to explore the effect on wake redirection, power, and loads. Also, although we uses a turbulent inflow wind, that wind had a quasi-static wind direction (i.e., the mean wind direction is fixed). In reality, the mean direction of the inflow wind is not locked exactly on a certain direction over time. More sophisticated wake-redirection methods are currently being explored by researchers at NREL, ECN, and the Delft University of Technology, and those methods would be explored

further. Such methods still rely upon yaw misalignment, but each turbine may have its own misalignment angle, further optimizing power output, and the methods can cope with mean wind direction changes over time. The proposed Fishermen's Atlantic City Windfarm is an ideal situation for simulation-in-the-loop experimentation and exploration of wakes and wake-redirection control.

Acknowledgements

This research was funded through the U.S. Department of Energy Offshore Wind Advanced Technology Demonstration Project. The research was performed using computational resources sponsored by the Department of Energy's Office of Energy Efficiency and Renewable Energy and located at the National Renewable Energy Laboratory.

Nomenclature

CFD	computational fluid dynamics
DNS	direct numerical simulation
ECN	Energy Centre of the Netherlands
IPC	individual pitch control
LES	large-eddy simulation
NREL	National Renewable Energy Laboratory
OOP	out of plane
RANS	Reynolds-averaged Navier-Stokes
RMS	root mean square
hr	hours
K	kelvin
km	kilometers
MW	megawatts
m	meters
m/s	meters per second
s	seconds

References

1. Fleming, P., Gebraad, P., Lee, S., van Wingerden, J. W., Johnson, K., Churchfield, M., Michalakes, J., Spalart, and P., Moriarty, P., "Evaluating Techniques for Redirecting Turbine Wakes Using SOWFA," International Conference on Aerodynamics of Offshore Wind Energy Systems and Wakes, Lyngby, Denmark, June 17–19, 2013.

2. Fleming, P., Gebraad, P., Lee, S., van Wingerden, J. W., Johnson, K., Churchfield, M., Michalakes, J., Spalart, P., and Moriarty, P., "High-Fidelity Simulation Comparison of Wake Mitigation Control Strategies for a Two-Turbine Case," International Conference on Aerodynamics of Offshore Wind Energy Systems and Wakes, Lyngby, Denmark, June 17–19, 2013.

3. Jiménez, Á., Crespo, A., and Migoya, E., "Application of a LES Technique to Characterize the Wake Deflection of a Wind Turbine in Yaw", *Wind Energy*, Vol. 13, No. 6, pp. 559 – 572, Sept. 2010.

4. Corten, P. G., Lindenburg, K., and Schaak, P., Inventors, Stichting Energieonderzoek Centrum Nederland (Energy Center of the Netherlands – ECN), Assignee, "Assembly of Energy Flow Collectors, Such as WindPark, and Method of Operation," United States Patent, No. US 7,299,627 B2, Nov. 27, 2007.

5. Corten, P. G., and Schaak, P., Inventors, Energieonderzoek Centrum Nederland (Energy Center of the Netherlands – ECN), Applicant, "Method and Installation for Extracting Energy From a Flowing Fluid," International Patent, World Intellectual Property Organization, No. WO 2004/111446 A1, Dec. 23, 2004.

6. Meneveau, C., Lund, T., Cabot, W., "A Lagrangian Dynamic Subgrid-Scale Model of Turbulence," *Journal of Fluid Mechanics*, Vol. 319, pp. 353 – 385, July 1996.

7. Sørensen, J. N., and Shen, W. Z., "Numerical Modeling of Wind Turbine Wake," *Journal of Fluids Engineering,* Vol. 124, pp. 393 – 399, June 2002.

8. "Atlantic City Offshore Windfarm Design Metocean Data," Ramboll, March 27, 2013.

9. Stull, R. B., *An Introduction to Boundary Layer Meteorology*, Kluwer Academic Publishers, 1988.